

*Short communication*

# Determination of Electrochemical Windows of Novel Electrolytes for Double Layer Capacitors by Stepwise Cyclic Voltammetry Experiments

Dominik Moosbauer,<sup>1</sup> Steffen Jordan,<sup>2</sup> Franz Wudy,<sup>1</sup>  
Sheng S. Zhang,<sup>3</sup> Michael Schmidt<sup>4</sup> and Heiner J. Gores<sup>1,\*</sup>

<sup>1</sup> University of Regensburg, Institute of Physical and Theoretical Chemistry,  
Universitaetsstrasse 31, D-93053 Regensburg, Germany

<sup>2</sup> Steffen Jordan, Infineon AG, Regensburg, Germany

<sup>3</sup> U.S. Army Research Laboratory, Sensors and Electron Devices Directorate, Adelphi,  
MD 20783-1197, USA

<sup>4</sup> Michael Schmidt, Merck KGaA, D-64271 Darmstadt, Germany

\* Corresponding author: E-mail: Heiner.gores@chemie.uni-regensburg.de

Received: 17-10-2008

Dedicated to Professor Josef Barthel on the occasion of his 80<sup>th</sup> birthday

## Abstract

In this work we synthesized two novel salts for electrochemical double layer capacitors, i.e. N,N-dimethylpyrrolidinium tetrakis(trifluoroacetato)borate (DMPBTFAc) and N-ethyl-N-methyl-pyrrolidinium bis[1,2-oxalato(2-O,O')]borate (EMPBOX), and determined the electrochemical window of their solutions in acetonitrile (AN) by using stepwise cyclic voltammetry. The electrochemical window plays an important role in electrochemical double layer capacitors (EDLCs) as the energy density of such devices depends on the square of the operating voltage. Because anodic and cathodic decomposition voltages may be shifted with respect to the open circuit voltage (OCV), the OCV is another important characteristic of such an electrolyte. Both DMPBTFAc and EMPBOX solutions show wide electrochemical windows of about 4 V with nearly equal voltage gaps for the anodic and cathodic decomposition at activated carbon electrodes.

**Keywords:** Double layer capacitor, EDLC, DLC, electrochemical window, cyclic voltammetry, Faradaic Fraction

## 1. Introduction

Currently, energy storage and transformation is an increasingly important issue. People would like to decrease their dependency on fossil fuels and tend more and more to renewable energy sources such as wind and solar energy. However strong fluctuations of energy feed-in into power networks can entail their collapse. To overcome these problems energy storage devices are needed. Electrochemical double layer capacitors (EDLCs) are great systems to store energy over a long time and release it later so, that strong fluctuations can be balanced. Furthermore, the interest in EDLCs for application in hybrid electric vehicles (HEVs) by combining them with batteries, fuel cells or

combustion engines<sup>1–3</sup> is increasing. In contrast to batteries, the EDLCs have low energy densities but they show very small time constants, and consequent high power densities<sup>4</sup>. The difference between batteries and EDLCs lies in the behavior of storing the electrical energy. In batteries Faradaic processes lead to storage of energy while in EDLCs two parallel capacitors, respectively one on each electrode, store charges. By polarization of an EDLC, two electrodes get contrarily charged. Under electric field, the anions and cations in the electrolyte are driven oppositely toward the surface of two electrodes and accumulated on the electrodes. With a very large electrode surface area of 1000 to 2500 m<sup>2</sup> g<sup>-1</sup><sup>5–8</sup> consisting in most cases of porous activated carbon (AC), the capacity *C* increases enor-

mously in comparison with usual electrolyte capacitors. This affects the storable energy  $E$  which is direct proportional to the capacity  $C$  and to the square of nominal voltage  $V$  of the capacitor, as shown by equation below:

$$E = \frac{1}{2} CV^2 \quad (1)$$

The maximal voltage that can be applied to an EDLC is limited by the electrochemical window of the electrolyte, for example, about 1.3 V for aqueous systems and about 2.5 V for non-aqueous solutions. Beyond the electrochemical window, the electrolyte decomposes. In cyclic voltammetry studies, the electrochemical window of electrolytes can be determined directly from an I-E response curve, however, for EDLC-electrodes the determination becomes more complicated. Whereas electrochemical windows of up to 5 V or even more on platinum (Pt) and glassy carbon (GC) electrodes are reported in reviews<sup>12</sup> for non-aqueous electrolytes, these show much lower windows in real EDLCs. The problem is due to the electrode surface area of the EDLCs. To get realistic values in comparison to real double layer capacitors, one cannot simply measure a cyclic voltammogram on Pt or GC working electrodes. Due to high capacitive currents caused by the porous and large electrode surface area of the activated carbon, the determination of electrochemical decomposing potentials at AC electrodes is very difficult. So Jow et al.<sup>9–11</sup> established a Faradaic Fraction to determine the electrochemical decomposing potential of electrolytes on these electrodes used in EDLCs. In this method, a single CV-scan is measured, increasing the final voltage stepwise and independently in anodic and cathodic directions. The method offers also a better determination of anodic and cathodic limits of the electrochemical windows and of the symmetry of the usable voltage range.

We developed a series of novel lithium electrolytes based on borates; for examples see Ref. 12 and our cited publications there. Currently the best performances of EDLCs have been obtained with tetraalkylammonium tetrafluoroborate in acetonitrile as solvent. When this solvent, which may be dangerous is substituted by solvents with low vapor pressure such as propylene carbonate (PC) other salts have to be used, due to the low solubility of tetraalkylammonium tetrafluoroborate in PC at low temperatures. Therefore we tried to combine our knowledge on ionic liquids with that on weakly coordinating anions based on borates<sup>13–17</sup> to obtain new electrolytes for EDLCs.<sup>18</sup> Finally, the determination of electrochemical windows is still a matter of debate.<sup>12</sup> With this paper we begin a series of studies based on proposed and new procedures to resolve open questions.

## 1. 1. Theoretical

In cyclic voltammetry measurement the Faradaic current  $i_f$  against an imposed potential is recorded. The

measured current describes the oxidation or reduction of the electrolyte and impurities, respectively. In the case of EDLCs with large electrode surface area, a second capacitive much larger current, the so-called non-Faradaic current  $i_{nf}$ , contributes to the total current  $i$ . The non-Faradaic current arises from charging and discharging of the double layer capacitor at the electrodes. Therefore, the total current is given by

$$i = i_f + i_{nf} \quad (2)$$

Because of the capacitive current  $i_{nf}$ , it is difficult to determine the decomposition of the electrolyte when an AC-electrode is used. To solve this problem, Jow et al.<sup>9–11</sup> proposed an alternative of the cyclic voltammetry measurement. To find the decomposition potential, several cyclic voltammograms are recorded stepwise by raising the first reverse potential after some cycles for a little amount. The obtained cyclic voltammogram is divided into two parts for the positive and negative potential scans, respectively. So the reductive and oxidative limit of the electrolyte is recorded in separate series of measurements.

To evaluate the decomposition potential, a Faradaic Fraction  $R$  is introduced and defined as the ratio of the charges  $Q_f$  and  $Q_{nf}$  of the Faradaic and non-Faradaic parts, respectively

$$R = \frac{Q_f}{Q_{nf}} \quad (3)$$

By splitting of every cyclic voltammogram through the line at  $i = 0$ , the Faradaic Fraction  $R$  can be calculated easily from the anodic charge  $Q_a$  and the cathodic charge  $Q_c$ , as shown below:

$$R = \frac{Q_a}{Q_c} - 1 \quad (4)$$

for the anodic part and for the cathodic part arises

$$R = \frac{Q_c}{Q_a} - 1 \quad (5)$$

By plotting the Faradaic Fraction  $R$  against the potential, a stability diagram of the electrolyte is obtained. If  $R$  exceeds 0.1 – a value proposed by Jow et al.<sup>9–11</sup> – the decomposition potential is reached and the electrochemical window of the electrolyte is determined by the resulting voltage range.

## 2. Experimental

### 2. 1. Acetonitrile

For every measurement we used acetonitrile (Selectipur®) by Merck KGaA (Darmstadt) as solvent. The water content was 20 ppm as checked by coulometric Karl

Fischer titration using a Mitsubishi Moisturemeter, Model CA-20. All solutions were prepared in a glove box (MBraun MB 150 BG and Mecaplex GB80) at low traces of water (< 1 ppm) and oxygen (< 2 ppm), by continuously monitoring with an H<sub>2</sub>O-Analyzer, Aquanal, company Kurt Gerhard, Blankenbach, and an O<sub>2</sub>-Analyzer from MBraun.

## 2. 2. Synthesis of DMPBTFAc

N,N-dimethylpyrrolidinium tetrakis(trifluoroaceto)borate (DMPBTFAc) was synthesized through one step by following the synthesis of the corresponding cesium salt of Harriss et al.<sup>19</sup>. To a solution of 0.60 mol boric acid (Merck, p.A.) and 0.60 mol dimethylpyrrolidinium trifluoroacetate in 300 mL dimethyl carbonate 1.43 mol of trifluoroacetato anhydride was added dropwise within 5 h at 10 °C. After reacting at 30 °C and stirring for 2 h, the reaction was completed by heating up to 70 °C for 12 h. The solution was concentrated in vacuum, followed by precipitating at –30 °C. The resulting precipitate was dried in vacuum at 60 °C for 12 h to give 0.59 mol of raw product that was recrystallized in diethyl ether at –30 °C and dried in ultra high vacuum (10<sup>–3</sup> mbar) at 70 °C for 48 h to obtain 0.39 mol of pure DMPBTFAc.

The purity was checked by <sup>1</sup>H-NMR (Table 1), <sup>13</sup>C-NMR (Table 2), <sup>11</sup>B-NMR, <sup>19</sup>F-NMR, and mass spec-

trometry. For all spectra 420 mg of DMPBTFAc in 1 mL acetonitrile-D<sub>3</sub> were used.

All analysis methods reflected the structure of DMPBTFAc without impurity lines. No peaks at 160 ppm were found which are related to acetate as impurity. <sup>11</sup>B-NMR showed an expected value at 1.01 ppm, only. The <sup>19</sup>F-NMR showed for fluorine a peak at –76.19 ppm with two <sup>13</sup>C-sattelites, <sup>1</sup>J = 285.8 Hz (F–CH<sub>2</sub>) and <sup>2</sup>J = 41.0 Hz (F–CO<sub>2</sub>). We observed an other peak at –75.17 ppm that could result from N,N-dimethylpyrrolidinium trifluoroacetate. However, integration of the peak yielded 0.03 %, only. Mass spectra analysis confirmed the correct product, too.

## 2. 3. Synthesis of EMPBOX

N-ethyl-N-methyl-pyrrolidinium bis[1,2-oxalato(2-O,O')]borate (EMPBOX) was synthesized according to the scheme shown in Figure 2. In the first step a solution of 0.3 mol iodoethane (Merck, p.A.) in 50 mL toluene was added dropwise at 80 °C to a solution of 0.197 mol 1-methylpyrrolidine (Fluka, puriss.) in 200 mL toluene. The mixture was heated up to 100 °C for 1 h and the resulting white precipitate N-ethyl-N-methyl-pyrrolidiniumiodide (EMPI) was dried in vacuum. The hydroxide EMPOH was obtained by an ion exchanger (Merck, Amberlite® IRA-410) that was freshly regenera-

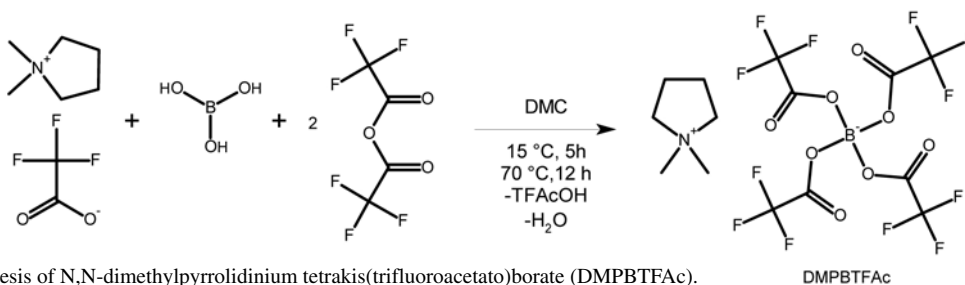


Figure 1: Synthesis of N,N-dimethylpyrrolidinium tetrakis(trifluoroacetato)borate (DMPBTFAc).

Table 1: <sup>1</sup>H-NMR data of DMPBTFAc.

ppm	Multiplicity	Assignment
3.46–3.40	m	α-CH <sub>2</sub>
3.06	s	CH <sub>3</sub>
2.20–2.12	m	β-CH <sub>2</sub>

Table 2: <sup>13</sup>C-NMR data of DMPBTFAc.

ppm	Multiplicity	J/Hz	Assignment	dept
156.32	q	41.1 ( <sup>13</sup> C– <sup>19</sup> F)	COO	0
118.22	s		acetonitrile	0
115.90	qq	285.8 ( <sup>13</sup> C– <sup>19</sup> F)	CF <sub>3</sub>	0
		4.2 ( <sup>13</sup> C– <sup>11</sup> B)		
66.87	t	2.9 ( <sup>13</sup> C– <sup>15</sup> N)	α-CH <sub>2</sub>	–
52.71	t	4.4 ( <sup>13</sup> C– <sup>15</sup> N)	CH <sub>3</sub>	+
22.59	s		β-CH <sub>2</sub>	–
1.7–0.5	m		acetonitrile	0

ted by a sodium hydroxide solution. In the third step 0.162 mol EMPOH was mixed with 0.162 mol boric acid and 0.334 mol oxalic acid dihydrate (Merck, p.A.). Using diethyl carbonate as the reacting medium, water was removed by azeotropic distillation. Thereby a yellow solution arises which crystallizes at –30 °C. The overlaying solution was withdrawn and frozen for a second time. The crystals were collected from both procedures followed by washing with dimethyl carbonate and drying at 45 °C in ultra high vacuum (10<sup>–3</sup> mbar). Yield: 0.1 mol of EMPBOX.

The purity was checked by <sup>1</sup>H-NMR (Table 3), <sup>13</sup>C-NMR (Table 4), <sup>11</sup>B-NMR, and mass spectrometry. For all spectra 170 mg of EMPBOX in 1 mL acetonitrile-D<sub>3</sub> was used.

The <sup>11</sup>B-NMR showed the expected peak at 8.1 ppm, only. The results confirm the high purity of the salt.

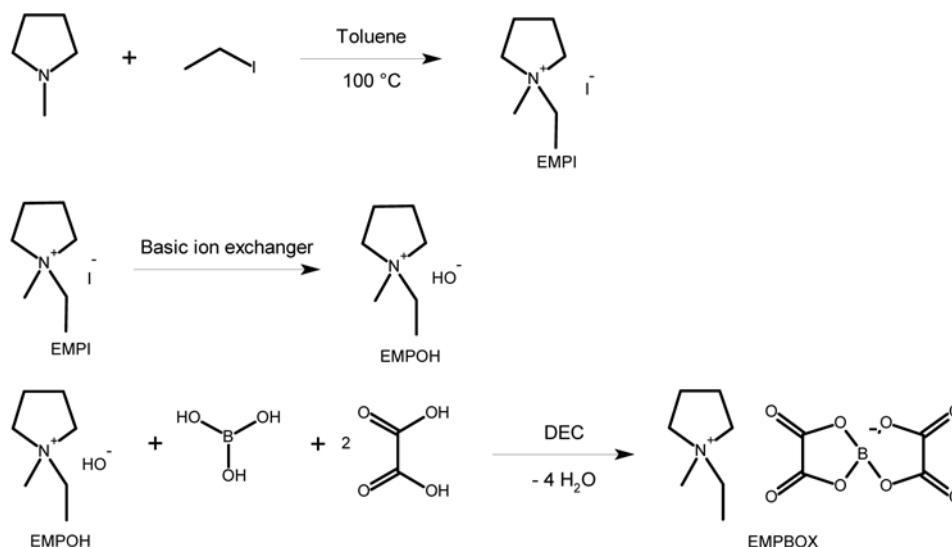


Figure 2: Synthesis of N-ethyl-N-methyl-pyrrolidinium bis[1,2-oxalato(2-O,O')]borate (EMPBOX).

Table 3: <sup>1</sup>H-NMR data of EMPBOX.

ppm	Multiplicity	J/Hz	Assignment
3.41	M		α-CH <sub>2</sub> -pyrrolidine
3.33	T	7.25 (CH <sub>2</sub> -CH <sub>3</sub> )	ethyl-CH <sub>2</sub>
2.94	S		methyl
2.15	M		β-CH <sub>2</sub> -pyrrolidine
1.94	M		acetonitrile
1.32	Tt	7.29 (CH <sub>3</sub> -CH <sub>2</sub> ) 2.05 (H-N)	ethyl-CH <sub>3</sub>

Table 4: <sup>13</sup>C-NMR data of EMPBOX.

ppm	Multiplicity	J/Hz	Assignment	dept
159.9	S		COO	/
118.5	S		acetonitrile	/
64.9	T	3.3 (C-N)	CH <sub>2</sub> -ethyl	-
60.5	T	2.9 (C-N)	β-CH <sub>2</sub> -pyrrole	-
48.7	T	4.4 (C-N)	α-CH <sub>2</sub> -pyrrole	-
22.4	s		CH <sub>3</sub> -methyl	+
9.6	s		CH <sub>3</sub> -ethyl	+
1.7	m		acetonitrile	

### 3. Results and Discussion

#### 3. 1. Oxidation and Reduction Stability of DMPBTFAc

All cyclic voltammetry measurements were carried out by an AutoLab's potentiostat / galvanostat PGSTAT30 (Eco Chemie / Metrohm, The Netherlands). To compare the electrochemical stability of DMPBTFAc against different materials, the electrochemical window was measured on three different working electrodes using a three-electro-

de cell. The cell was filled with the electrolyte in the Ar-Glovebox to avoid water and air impurities, and was sealed air-tightly, so that the measurement could be run in air.

The first measurement was done on a glassy carbon (GC, by Metrohm) working electrode using a Pt-sheet as the counter electrode and an Ag/AgNO<sub>3</sub> – Cryptand as the reference electrode.<sup>20–22</sup> This non-aqueous reference electrode is comparable to the saturated calomel electrode (SCE) for aqueous systems where the potential is stable due to assisting equilibria (on the one hand saturated KCl and a scarcely soluble salt on the other hand an excess of complexed silver ions and an excess of complexing agent, the cryptand). It is based on the work of Pleškov<sup>23</sup> and was proposed by Izutsu et al. It is currently our most preferred electrode,<sup>13,14,24</sup> if it can be used. Sometimes this electrode may not be used, e. g. if silver ions oxidize constituents of the studied solution.

Figure 3 shows cyclic voltammograms of a 1.2 M DMPBTFAc-AN solution on a GC and an Al electrode, respectively. On the GC electrode, the current densities are low until at 1.5 V where a sharp increase appears which is assumed to be caused by the anodic decomposition of the electrolyte. In cathodic direction a peak at about -1.4 V is observed, which is due to water impurities. When the working electrode was changed to an Al-strip with a surface area of 0.15 cm<sup>2</sup>, a cyclic voltammogram was recorded that is shown in Figure 3 by the dashed line. There are enormous differences in the cyclic voltammograms between GC and Al electrodes. The reductive sides are similar. But at the oxidative side the current density on the Al electrode is much higher than on the GC electrode. The decomposition begins at a much lower potential (about 1.0 V). This means that the decomposition potential is about 0.5 V lower than the one observed on the GC working electrode. This behavior may be caused by

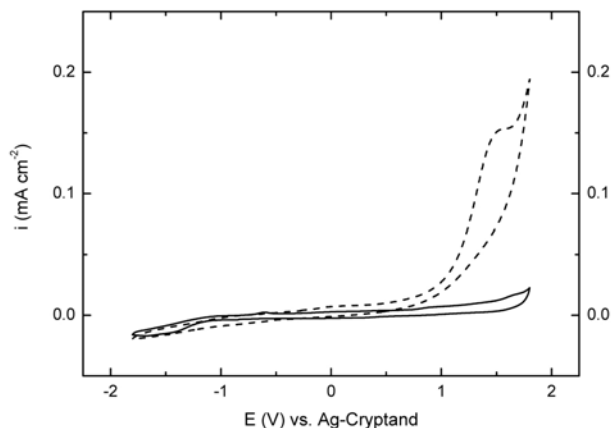


**Figure 3:** Cyclic voltammograms of a 1.2 M DMPBTFAc-AN solution which were recorded from 2<sup>nd</sup> cycle at a scanning rate  $v$  of 5  $\text{mVs}^{-1}$ ; — on GC, -- on Al-strip.

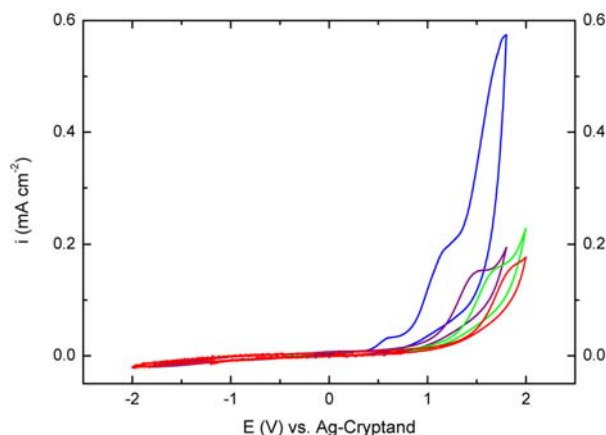


**Figure 5:** Cyclic voltammograms of a 1.2 M DMPBTFAc-AN solution on GC; ■ 1<sup>st</sup> scan, ■ 2<sup>nd</sup> scan, ■ 3<sup>rd</sup> scan, ■ 4<sup>th</sup> scan; scanning rate  $v = 5 \text{ mVs}^{-1}$

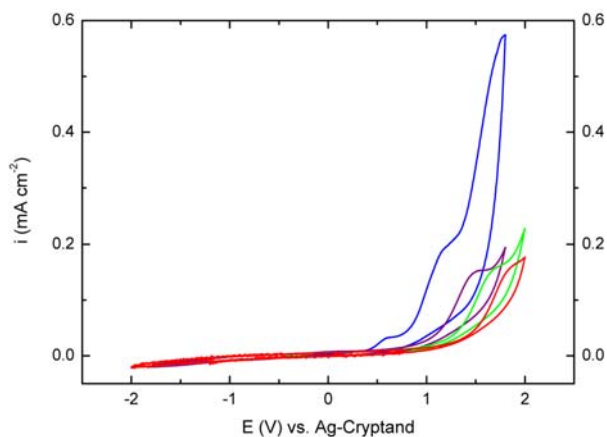


**Figure 4:** Cyclic voltammograms of a 1.2 M DMPBTFAc-AN solution on an Al-strip electrode ■ 1<sup>st</sup> scan, ■ 2<sup>nd</sup> scan, ■ 3<sup>rd</sup> scan, ■ 4<sup>th</sup> scan; scanning rate  $v = 5 \text{ mVs}^{-1}$

the anodic oxidation of aluminum, see also Figure 4, where several scans are shown.

With increasing cycle numbers we observed a decrease of the oxidative currents above 1.0 V. After the first cycle the current densities decreased more than factor two and reached approximately the same current values in further cycles, but at higher potentials. That shows an increasing passivation of the Al-strip electrode. In contrast, the measured current densities for cyclic voltammetry measurements of DMPBTFAc on GC electrode are very small and mainly overlapping for four cycles, see Figure 5, showing again that high currents at Al-electrodes are caused by corrosion of aluminum and subsequent passivation.

To obtain comparable results with realistic behavior in EDLCs, we measured the electrochemical window according to the method by Jow et al.<sup>9–11</sup> For this measurement, a 1.0 M DMPBTFAc-AN solution was used. As re-

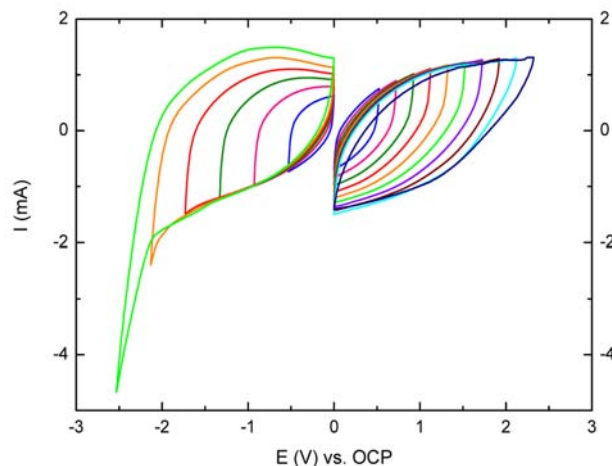


**Figure 6:** Cyclic voltammograms of a 1.0 M DMPBTFAc-AN solution on AC; scanning rate  $v = 5 \text{ mVs}^{-1}$

ference electrode the  $\text{Ag}/\text{AgNO}_3$  – cryptand electrode was applied. The counter and working electrodes were two identical activated carbon electrodes coated on an Al substrate, which were previously dried in vacuum for a week. This material is used in real EDLCs too. The first reverse potentials were increased stepwise after ten cycles. As the start potential used was the pre-determined open circuit voltage (OCV) applied.

Figure 6 shows that the cyclic voltammograms are clearly distinguished from the two diagrams in Figure 3. There is no zero-current region to be recognized but charging and discharging currents of the capacitor's double layer. When exceeding a critical potential, the cyclic voltammogram gets more and more asymmetrical. At this potential the electrolyte begins to decompose. Furthermore at higher negative potentials the activated carbon detaches from the Al supporting which destroys the working electrode. For a more precise definition of the de-

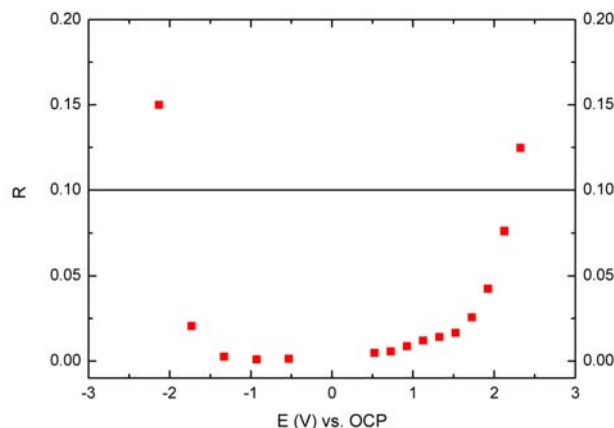


**Figure 7:** Faradaic Fraction  $R$  as a function of the potential for a 1 molal DMPBTFAc-AN solution on AC electrode; ■ Faradaic Fraction  $R$ , — limit according to Jow, for details see text.

composition potential we calculated the Faradaic Fraction  $R$ .

Figure 7 shows the electrochemical window of a 1 M DMPBTFAc-AN solution against the activated carbon electrode. It is shown that the value of  $R$  is gradually increased either with an increase in the potential on anodic scanning or with a decrease in the potential on cathodic scanning. By linear interpolation at the limit for  $R = 0.1$ , the decomposition potential of the electrolyte is determined. For this system, a reductive decomposition potential of  $-2.0$  V is obtained, and an oxidative limit of  $2.2$  V is reached. The resulting slightly asymmetric potential window is  $4.0$  V only, and not  $4.2$  V because of the smaller and hence limiting reductive potential.

These results indicated that the oxidative decomposition potential of the DMPBTFAc-AN solution is significantly affected by the type of electrodes. The oxidative decomposition potential is ranged from  $1.0$  V (Al-strip) through  $1.5$  V (GC) to more than  $2.2$  V at the activated carbon electrode.

### 3. 2. Oxidation and Reduction Stability of EMPBOX

The method of Jow et al.<sup>9–11</sup> was also used to determine the stability of EMPBOX. Again, an Ag/AgNO<sub>3</sub>-Cryptand electrode served as the reference electrode. As the counter and working electrode, the activated carbon coated on aluminum was used.

The cyclic voltammetry of EMPBOX showed an electrochemical window ranging from  $-1.8$  V to more than  $+2.0$  V. Also here the destruction of the working electrode's surface resulted in strong reductive and irreversible currents. The resulting electrochemical window is limited by the reductive and oxidative decomposing potentials of the electrolyte and it was determined to be  $3.6$  V.

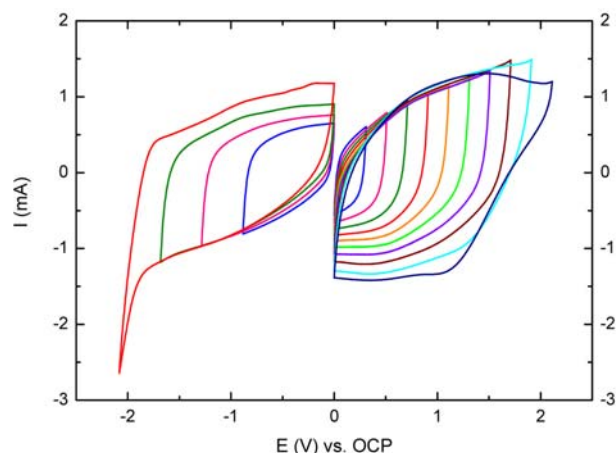


**Figure 8:** Cyclic voltammograms of a  $0.67$  M EMPBOX-AN solution on AC;  $v = 5$  mVs<sup>-1</sup>.

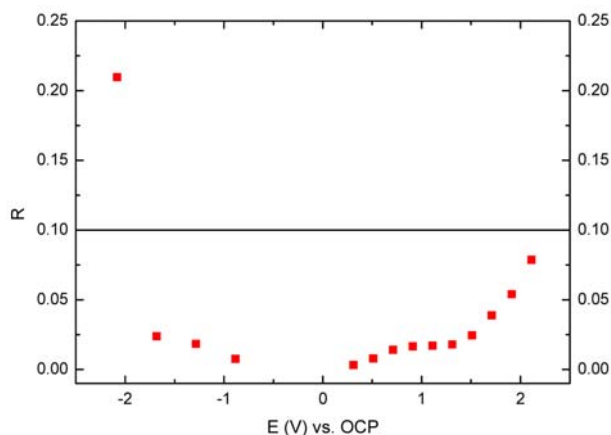


**Figure 9:** Stability diagram of a  $0.67$  M EMPBOX-AN solution on an AC electrode; ■ Faradaic Fraction  $R$ , – limit according to Jow.

## 4. Conclusions

The cyclic voltammetry results show that the choice of the working electrode is very important. For a good comparison with commercial EDLCs, it is necessary to use the same material to simulate realistic cells. Many factors affect the behavior of the electrolyte. The material and surface area of the electrodes have a huge influence on the current behavior. It is shown that plane electrodes such as GC or Al-strips result in a wider electrochemical window. In contrast, a porous electrode such as activated carbon with a huge surface area complicates the determination of electrochemical windows due to its overlaying capacitive charge and discharge. By plotting the Faradaic Fraction  $R$  against electrode potential, it is possible to determine anodic and cathodic decomposing potentials of the electrolyte on a porous activated carbon electrode. The electrochemical window on an activated carbon elec-

trode was determined to be about 4.0 V for DMPBTFAc-AN and 3.6 V for EMPBOX-AN solutions, respectively. These values are higher than normal operating voltages of EDLCs reported ever. Hence, both salts can be expected to be very suitable for practical applications in commercial EDLCs. It is interesting to stress that DMPBTFAc, in contrast to EMPBOX, entails a corrosion of aluminum, followed by the formation of a passivation film, as shown by the difference in consecutively scanned CVs at Al and GC electrodes. This result means that the voltage decay is much larger in an EDLC filled with DMPBTFAc-AN solutions after first charging. This unwanted effect should gradually disappear with the passivation of aluminum.

Finally we suggest the use of a lower R-limit than that introduced by Jow et al. In future papers we will discuss this issue by comparing electrochemical voltage windows determined using different *R* ratios compared with results from real capacitors filled with the electrochemically studied solutions. Our preliminary results have shown that *R* should be reduced to 0.02 or even 0.01 in order to get comparable results from electrochemical measurements and real EDLCs.

## 5. Acknowledgments

We thank Prof. Dr. J. Barthel for his continued interest in the work of our workgroup, Electrochemistry and Electrolytes, based on his previous work and his support for over forty years. Thanks also go to our industrial partners Merck KGaA (Darmstadt, Germany) and Epcos (Heidenheim an der Brenz, Germany) for funding our work and to Dirk Herrmann for editing.

## 6. References

1. E. Faggioli, P. Rena, V. Danel, X. Andrieu, R. Mallant, H. Kahlen, *J. Power Sources* **1999**, *84*, 261–269.
2. M. Mastragostino, F. Soavi, *J. Power Sources* **2007**, *174*, 89–93.
3. W. G. Pell, B. E. Conway, W. A. Adams, J. de Oliveira, *J. Power Sources* **1999**, *80*, 134–141.
4. B. E. Conway, *Electrochemical Supercapacitors*, Kluwer Academic/Plenum, **1999**.
5. A. G. Pandolfo, A. F. Hollenkamp, *J. Power Sources* **2006**, *157*, 11–27.
6. T. Osaka, X. Liu, M. Nojima, T. Momma, *J. Electrochem. Soc.* **1999**, *146*, 1724–1729.
7. H. Shi, *Electrochim. Acta* **1996**, *41*, 1633–1639.
8. P. Taberna, P. Simon, J. Fauvarque, *J. Electrochem. Soc.* **2003**, *150*, A292–A300.
9. K. Xu, S. P. Ding, T. R. Jow, *J. Electrochem. Soc.* **1999**, *146*, 4172–4178.
10. K. Xu, M. S. Ding, T. R. Jow, *J. Electrochem. Soc.* **2001**, *148*, A267–A274.
11. K. Xu, M. S. Ding, T. R. Jow, *Electrochim. Acta* **2001**, *46*, 1823–1827.
12. J. Barthel, H. J. Gores, *Handbook of Battery Materials*, Wiley-VCH, Weinheim, NY, **1999**.
13. M. Zistler, P. Wachter, P. Wasserscheid, D. Gerhard, A. Hinsch, R. Sastrawan, H. J. Gores, *Electrochim. Acta* **2006**, *52*, 161–169.
14. M. Zistler, P. Wachter, C. Schreiner, M. Fleischmann, D. Gerhard, P. Wasserscheid, A. Hinsch, H. J. Gores, *J. Electrochem. Soc.* **2007**, *154*, B925–B930.
15. T. Herzig, C. Schreiner, H. Bruggachner, S. Jordan, M. Schmidt, H. J. Gores, *J. Chem. Eng. Data* **2008**, *53*, 434–438.
16. M. Amereller, M. Multerer, C. Schreiner, J. Lodermeier, A. Schmid, J. Barthel, H. J. Gores, *J. Chem. Eng. Data* **2008**, (in print), available online. Web Release Date: 11-Oct-2008; DOI: 10.1021/je800473h
17. C. Schreiner, M. Amereller, H. J. Gores, *Chemistry, A European Journal*, in print, <http://dx.doi.org/10.1002/chem.200802243>.
18. H. Bruggachner, S. Jordan, M. Schmidt, W. Geissler, A. Schwake, J. Barthel, B. E. Conway, H. J. Gores, *J. New Mater. Electrochem. Syst.* **2006**, *9*, 209–220.
19. M. G. Harriss, J. B. Milne, *Can. J. Chem.* **1971**, *49*, 3612–3616
20. K. Izutsu, *Electrochemistry in Nonaqueous Solutions*, Wiley-VCH, Weinheim, **2002**.
21. K. Izutsu, M. Ito, E. Sarai, *Anal. Sci.* **1985**, *1*, 341–344.
22. A. Lewandowski, A. Szukalska, M. Galinski, *New J. Chem.* **1995**, *19*, 1259–1263.
23. W. A. Pleskow, *J. Phys. Chem.* **1948**, *22*, 351–361.
24. H. Bruggachner, Dissertation, Universität Regensburg, **2004**.

## Povzetek

Sintetizirali smo dne novi spojini, primerni za uporabo v dvoplastnih kondenzatorjih: N,N-dimetilpirolidinijev tetrakis(trifluoroacetat)borat (DMPBTFAc) in N-etil-N-metil-pirolidinijev bis[1,2-oksalat(2-O,O')]borat (EMPBOX). Za raztopine obeh spojin v acetonitrilu (AN) smo s ciklično voltmetrijo določili elektrokemijsko okno, ki igra pomembno vlogo v dvoplastnih kondenzatorjih. Njihova energijska gostota je namreč odvisna od kvadratnega korena delovne napetosti. Anodna in katodna razkrojna napetost sta lahko premaknjeni glede na napetost odprtega kroga, ki je pomembna karakteristika elektrolita. Raztopine DMPBTFAc in EMPBOX v AN kažejo široko elektrokemijsko okno (4 V) s približno enako katodno in anodno razkrojno napetostjo na aktiviranih ogljikovih elektrodah.